

THE EVOLUTION OF STELLAR ROTATION AND THE HYDROGEN ATMOSPHERES OF HABITABLE-ZONE TERRESTRIAL PLANETS

C. P. JOHNSTONE¹, M. GÜDEL¹, A. STÖKL¹, H. LAMMER², L. TU¹, K. G. KISLYAKOVA², T. LÜFTINGER¹, P. ODERT²,
N. V. ERKAEV^{3,4}, E. A. DORFI¹

¹University of Vienna, Department of Astrophysics, Vienna, Austria

²Space Research Institute, Austrian Academy of Sciences, Graz, Austria

³Institute for Computational Modelling, Siberian Division of Russian Academy of Sciences, Krasnoyarsk, Russian Federation

⁴Siberian Federal University, Krasnoyarsk, Russian Federation

(Dated: March 13, 2018)

Draft version March 13, 2018

ABSTRACT

Terrestrial planets formed within gaseous protoplanetary disks can accumulate significant hydrogen envelopes. The evolution of such an atmosphere due to XUV driven evaporation depends on the activity evolution of the host star, which itself depends sensitively on its rotational evolution, and therefore on its initial rotation rate. In this letter, we derive an easily applicable method for calculating planetary atmosphere evaporation that combines models for a hydrostatic lower atmosphere and a hydrodynamic upper atmosphere. We show that the initial rotation rate of the central star is of critical importance for the evolution of planetary atmospheres and can determine if a planet keeps or loses its primordial hydrogen envelope. Our results highlight the need for a detailed treatment of stellar activity evolution when studying the evolution of planetary atmospheres.

Subject headings: planets and satellites: atmospheres – planets and satellites: terrestrial planets – planet-star interactions – stars: activity – stars: low-mass – stars: rotation

1. INTRODUCTION

Planetary atmospheres evolve under the influence of the winds and high energy radiation of their hosts stars. High-energy radiation drives chemistry (Tian et al. 2008; Koskinen et al. 2013; Shaikhislamov et al. 2014; Shematovich et al. 2014; Chadney et al. 2015) and heating, causing expansion and mass loss (Tian et al. 2005; Erkaev et al. 2013; Luger et al. 2015). In addition, atmospheres exposed to stellar winds often experience significant additional loss (Lammer et al. 2007; Lichtenegger et al. 2010; Lundin 2011; Kislyakova et al. 2013).

Atmospheric evolution is fundamentally linked to the evolution of stellar winds and XUV emission (where XUV is X-ray+EUV). A star’s XUV emission originates from magnetically heated chromospheric and coronal plasma (Güdel 2004; Jardine et al. 2006) and is determined primarily by the star’s rotation, with rapid rotators being more active than slow rotators, except at rapid rotation where the activity saturates (Wright et al. 2011). As a star ages, its activity declines due to spin-down (Güdel et al. 1997; Vidotto et al. 2014). Due to the fact that a star’s rotation evolves differently depending on its initial rotation rate, a star’s activity level is *not* uniquely determined by its mass and age (Johnstone et al. 2015a; Tu et al. 2015). Solar mass stars at ages of 1 Myr have a large distribution of rotation rates, ranging from a few to a few tens of times faster than the current solar rotation rate (Herbst et al. 2002; Bouvier et al. 2014; Matt et al. 2015). At this age, due to their internal structures, all stars lie above the saturation threshold in rotation. Tu et al. (2015) found that the age at which a star falls out of saturation varies between ~ 10 Myr and several hundred Myr depending on its initial rotation rate.

The simplest planetary atmospheres are those domi-

nated by hydrogen collected from the circumstellar disk (Lammer et al. 2014; Stökl et al. 2015). For such an atmosphere to form, the planet must grow to a significant mass ($>0.1 M_{\oplus}$) before the disk dissipates. Disk lifetimes are typically a few Myr (Kraus et al. 2012), whereas standard planet formation theory suggests that terrestrial planet formation takes much longer (Lunine et al. 2011). However, the existence of low density terrestrial planets, such as those in the Kepler-11 system (Lissauer et al. 2011), suggest that at least some terrestrial planets are able to form in the gas disk. Furthermore, recent studies have indicated that a large fraction of observed terrestrial planets have low densities, suggesting that they have thick gaseous envelopes (Marcy et al. 2014; Rogers 2015).

The capture and subsequent escape of disk gas by terrestrial planets was studied by Lammer et al. (2014) who modeled the first 100 Myr of the planet’s life and assumed the star’s activity remains saturated for the entire time. The amount of disk gas captured is strongly dependent on the core mass, with low mass cores capturing orders of magnitude less gas than high mass cores. Lammer et al. (2014) showed that low-mass habitable-zone terrestrial planets will not keep hydrogen envelopes for evolutionary timescales, whereas many high-mass terrestrial planets will always keep such atmospheres. While the planet is embedded in the disk, thermal pressure from disk gas on the atmosphere provides additional support binding it to the core. Stökl et al. (2015) showed that when this thermal support is removed, the atmosphere can flow away at rates that also strongly depend on core mass.

In this letter, we study the importance of the initial stellar rotation rate on the XUV driven evolution of hydrogen atmospheres. In Section 2, we describe our model for atmospheric evolution; in Section 3, we calculate models for a range of cases; in Section 4, we discuss

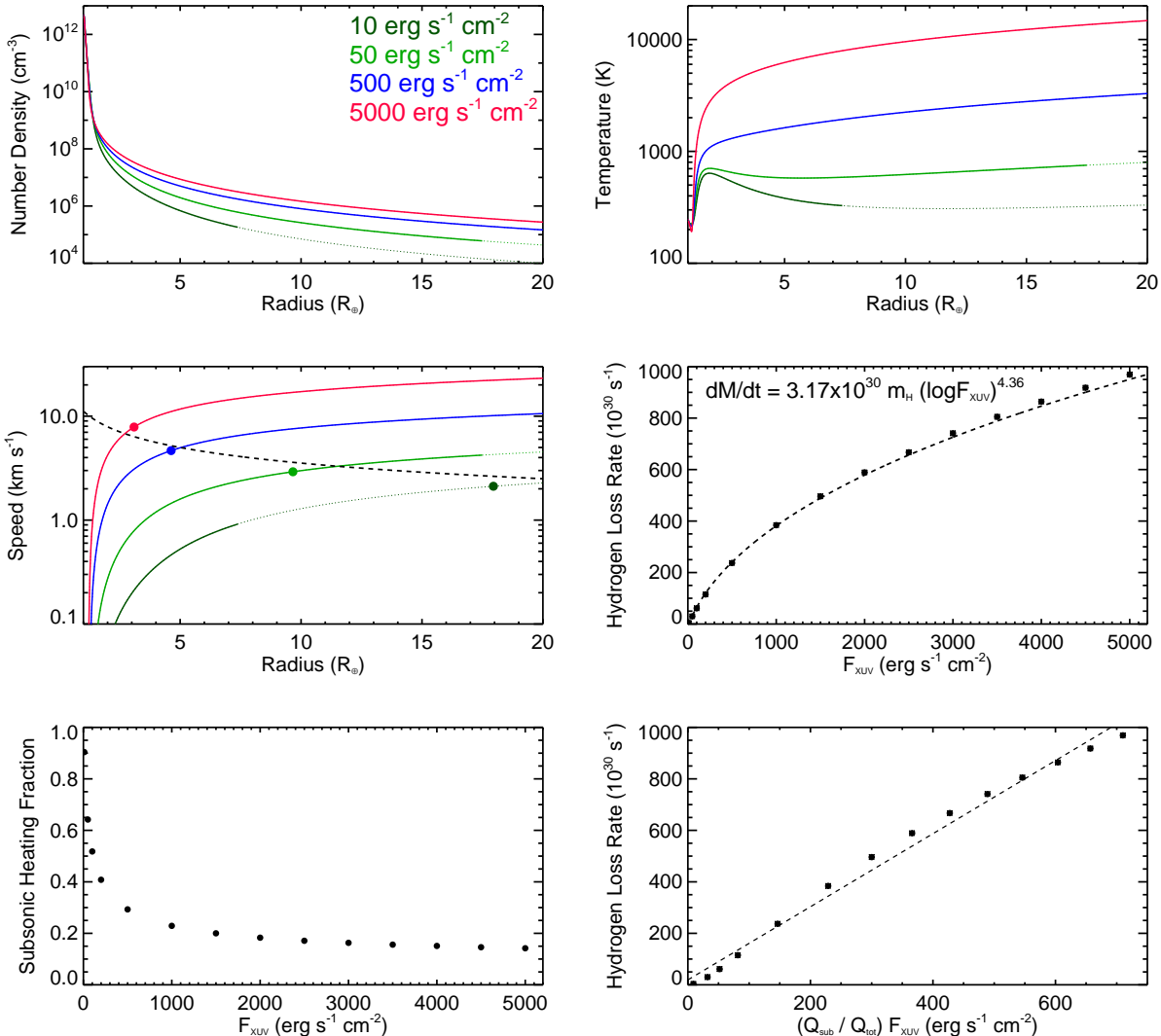


FIG. 1.— Hydrodynamic models of upper atmosphere expansion from an Earth mass planet with different input XUV fluxes. For F_{XUV} of 10, 50, 500, and 1000 $\text{erg s}^{-1} \text{cm}^{-2}$, we show profiles of hydrogen density (*upper-left*), temperature (*upper-right*), and radial expansion velocity (*middle-left*). The dotted parts of the lines show the regions where the Knudsen number (defined here using Eqn. 3-5 of Erkaev et al. 2015) is greater than unity, and therefore the simulations are not reliable (the top of the solid line therefore shows the exobase). In the velocity plot, the dashed line is the escape velocity and the circles show where the wind becomes supersonic. *Middle-right panel*: atmospheric hydrogen loss rate as a function of F_{XUV} . *Lower-left panel*: subsonic heating fraction (i.e. the fraction of heat deposited below the sonic point), $Q_{\text{sub}}/Q_{\text{tot}}$, as a function of input F_{XUV} . *Lower-right panel*: \dot{M}_{at} as a function of $(Q_{\text{sub}}/Q_{\text{tot}})F_{\text{XUV}}$, showing that the \dot{M}_{at} is approximately proportional to the energy deposited in the subsonic part of the wind.

our results.

2. ATMOSPHERIC EVOLUTION MODEL

Our atmospheric evolution calculations combine a hydrodynamic upper atmosphere model (Section 2.1), a hydrostatic lower atmosphere model (Section 2.2), and evolutionary tracks for stellar XUV luminosity (Section 2.3). In all models, we assume the planet is in the habitable zone at 1 AU around a solar mass star and has an equilibrium temperature of 250 K. We therefore do not consider the evolutionary changes in the star’s bolometric luminosity, which will be studied in future work.

2.1. Atmospheric mass loss and the F_{XUV} dependence

To predict the atmospheric mass loss rate, \dot{M}_{at} , we use hydrodynamic upper atmosphere simulations performed

using the Versatile Advection Code (VAC; Tóth 1996). We run our simulations in 1D spherical geometry with 1000 unevenly spaced grid cells and include the planet’s gravity and XUV heat deposition. At the base of the simulation, we assume a constant density of $5 \times 10^{12} \text{cm}^{-3}$ and a constant temperature of 250 K. The base density was chosen so that the entire XUV flux will be absorbed within the computational domain. We further assume that the upper atmosphere consists purely of neutral atomic hydrogen. The three input parameters are the planetary mass, M_{pl} , the stellar XUV energy flux, F_{XUV} , and the radius of the base of the simulation, R_0 (alternatively, we often use $z_0 = R_0 - R_{\text{core}}$).

We assume that mass loss happens evenly over the entire area of the planet, excluding the shadow cast by the planet itself (i.e. over $\sim 3\pi$ steradians). We average

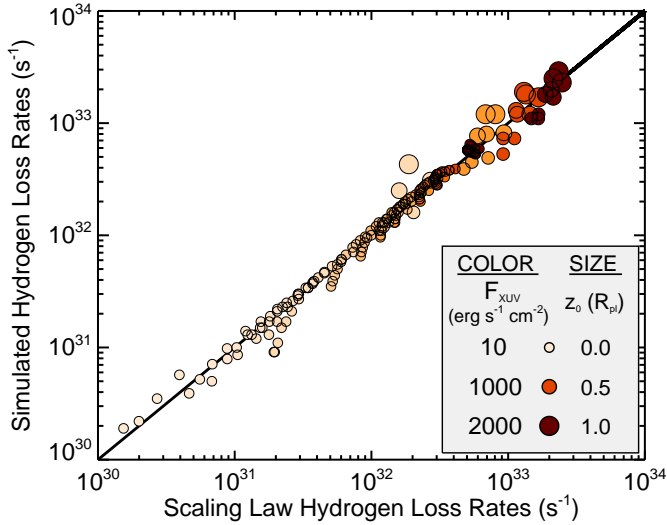


FIG. 2.— Simulated \dot{M}_{at} from our hydrodynamic simulations against values from our scaling law (Eqn. 1). Each symbol represents one simulation, with darker colours showing larger F_{XUV} and larger symbols showing larger z_0 .

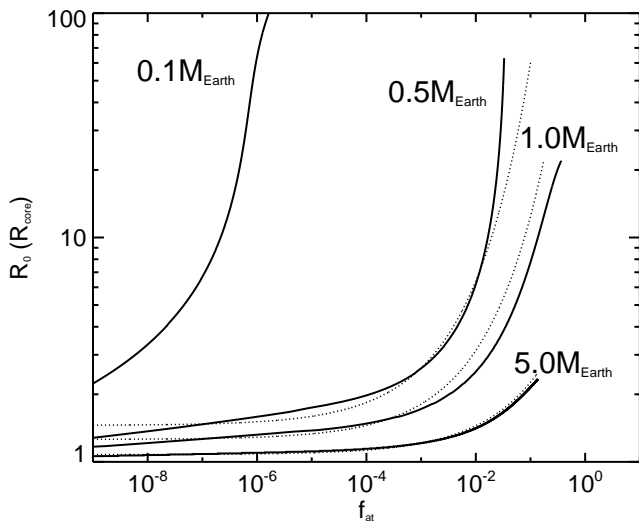


FIG. 3.— The value of R_0 ($= R_{\text{core}} + z_0$) as a function of planetary atmospheric mass, $f_{\text{at}} = M_{\text{at}}/M_{\text{pl}}$, for different planetary masses. The dotted lines show the approximate values of R_0 given by Eqn. 3.

the total input flux over this area, which gives an input XUV flux at the top of the simulations of $F_{\text{XUV}}/3$. As in Murray-Clay et al. (2009) and Erkaev et al. (2013), we assume a single wavelength for all photons and use the absorption cross section from Erkaev et al. (2013) of $\sigma = 5 \times 10^{-18} \text{ cm}^2$. We integrate the input XUV flux downwards through the atmosphere by decreasing the radiation flux by a factor of $e^{-\tau}$ when traveling through each grid cell, where $\tau = n\sigma ds$, ds is the grid cell thickness, and n is the hydrogen atom number density. The heating of the gas within each grid cell is given by $q = \epsilon n F_{\text{XUV}}$, where F_{XUV} is in this case the XUV flux in the grid cell and $\epsilon = 0.15$ is the heating efficiency parameter (Shematovich et al. 2014; Erkaev et al. 2015;

Ionov & Shematovich 2015).

To test the dependence of \dot{M}_{at} on F_{XUV} , we run 14 models for Earth mass planets with $z_0 = 100 \text{ km}$ and F_{XUV} ranging from 10 to $5000 \text{ erg s}^{-1} \text{ cm}^{-2}$. The current Earth receives an F_{XUV} of $\sim 5 \text{ erg s}^{-1} \text{ cm}^{-2}$. For very similar simulations and F_{XUV} of 10, 50, and 100 erg s^{-1} , Erkaev et al. (2013) found hydrogen atom loss rates of 5.0×10^{30} , 1.9×10^{31} , and $3.2 \times 10^{31} \text{ s}^{-1}$. We find similar values of 4.5×10^{30} , 3.0×10^{31} , and $6.1 \times 10^{31} \text{ s}^{-1}$.

The results of our 14 simulations are demonstrated in Fig. 1. Clearly, \dot{M}_{at} does not depend linearly on F_{XUV} because as F_{XUV} increases, the fraction of the input energy available to lift mass away from the planet decreases. In our models, \dot{M}_{at} is only influenced by heating below the sonic point. As F_{XUV} increases, the sonic point moves closer to the planet leading to a smaller fraction of the energy being deposited in the subsonic region. A similar effect can be seen in hydrodynamic stellar wind models (e.g. see Fig. 8 and Fig. 9 of Johnstone et al. 2015b).

To derive a scaling law for \dot{M}_{at} , we run a grid of models with a range of M_{pl} , F_{XUV} , and z_0 . In total, we run 230 simulations with M_{pl} between 0.5 and $5.0 M_{\oplus}$, F_{XUV} between 10 and $2000 \text{ erg s}^{-1} \text{ cm}^{-2}$, and z_0 between 100 km and $1 R_{\text{core}}$. Of these simulations, 46 did not give realistic results due to numerical difficulties. Motivated by experiments with different functions, we assume that \dot{M}_{at} is given by

$$\dot{M}_{\text{at}} = a m_{\text{H}} M_{\text{pl}}^b z_0^c (\log F_{\text{XUV}})^{g(M_{\text{pl}}, z_0)}, \quad (1)$$

where

$$g(M_{\text{pl}}, z_0) = d M_{\text{pl}}^e z_0^f, \quad (2)$$

m_{H} is the mass of a hydrogen atom and $z_0 = R_0 - R_{\text{core}}$ is the altitude of the base of the simulation. We find that $a = 1.858 \times 10^{31}$, $b = -1.526$, $c = 0.464$, $d = 4.093$, $e = 0.249$, and $f = -0.022$; in addition, M_{pl} , z_0 , and F_{XUV} must be in units of M_{\oplus} , R_{\oplus} , and $\text{erg s}^{-1} \text{ cm}^{-2}$. The quality of this fit to our grid of simulations is shown in Fig. 2. Although our scaling law is inelegant and gives little intuitive insight into the physics of evaporation, it likely gives good estimates of \dot{M}_{at} .

2.2. Lower atmospheric extent

The extent of a planet's atmosphere is strongly influenced by the planet's mass, the atmospheric mass, and the atmospheric composition (Mordasini et al. 2012; Howe et al. 2014; Lopez & Fortney 2014). Based on a few simplifying assumptions, we are able to estimate z_0 from the planetary and atmospheric masses. In general, in more massive atmospheres, z_0 is at higher altitudes, leading to higher \dot{M}_{at} . As an atmosphere evaporates, both z_0 and \dot{M}_{at} decrease; when the atmosphere is gone, $z_0 = 0$ and Eqn. 1 predicts no mass loss.

The exact definition of z_0 is the altitude at which the hydrogen atom number density is $5 \times 10^{12} \text{ cm}^{-3}$, since that is what we take as the density at the base of our simulations. Calculating z_0 therefore requires the lower atmosphere density structure. For this, we use the initial model integrator of the TAPIR-Code (Stökl 2008; Stökl et al. 2015) to solve the hydrostatic structure equations (Eqn. 4-6 of Stökl et al. 2015) taking into ac-

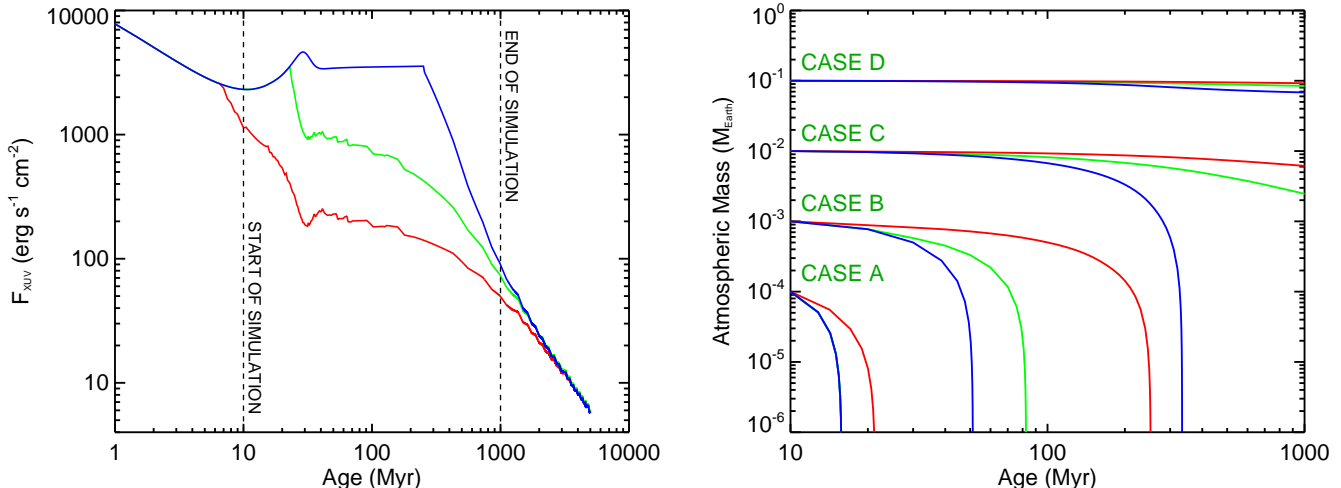


FIG. 4.— *Left panel:* the evolution of the XUV (1-960Å) flux received by a planet orbiting a solar mass star at 1 AU assuming separately that the star is a slow rotator (red), an average rotator (green), and a fast rotator (blue). *Right panel:* the evolution of hydrogen protoatmospheres between 10 Myr and 5 Gyr in response to the XUV irradiation for Earth mass planets. The four cases, marked as green symbols in Fig. 5, correspond to different initial atmospheric masses.

count radiative and convective energy transport. We assume that the core density is equal to that of the Earth for all bodies, meaning that $R_{\text{core}} \propto M_{\text{pl}}^{1/3}$. To describe the gas in the lower atmosphere, we use the equation of state derived by Saumon et al. (1995) for a hydrogen and helium mixture, and the opacities for gas and dust from Freedman et al. (2008) and Semenov et al. (2003), respectively. The free parameters are the flux of energy from the planetary core, L_{pl} , and the dust depletion factor, f . As in Stökl et al. (2015), we take $L_{\text{pl}} = 10^{21} (M_{\text{pl}}/M_{\oplus}) \text{ erg s}^{-1}$ and $f = 0.01$. In reality, these two parameters depend on the specific planet formation scenario and on the age of the system; a more detailed treatment of these parameters will be the subject of further work.

The dependence of R_0 on planetary and atmospheric masses are shown in Fig. 3. For masses above $0.5M_{\oplus}$, this dependence is approximately described by

$$\log\left(\frac{R_0}{R_{\text{core}}}\right) = (2.5f_{\text{at}}^{0.4} + 0.1) \left(\frac{M_{\text{pl}}}{M_{\oplus}}\right)^{-0.7}. \quad (3)$$

The dotted lines in Fig. 3 show the quality of this fit. The mass dependent upper limit for f_{at} , i.e. the value at which the lines in Fig. 3 turn upwards, is given by

$$f_{\text{at,max}} \approx 0.3 \left(\frac{M_{\text{pl}}}{M_{\oplus}}\right)^{3.6}. \quad (4)$$

For a hydrogen atmosphere of a terrestrial planet, \dot{M}_{at} can easily be estimated by combining Eqn. 1 with Eqn. 3, though our scaling laws only apply to planets with equilibrium temperatures of ~ 250 K.

2.3. Stellar XUV evolution

Tu et al. (2015) developed a rotational evolution model for solar mass stars at the 10th, 50th, and 90th percentiles of the rotational distributions based on the models of Gallet & Bouvier (2013) and Johnstone et al. (2015a). Tu et al. (2015) combined their rotation

tracks with an empirical relation between rotation and L_X (5-100Å) derived by Wright et al. (2011), and the conversion between L_X and L_{EUV} (100-920Å) derived by Sanz-Forcada et al. (2011), to predict evolutionary tracks for L_X and L_{EUV} . For the pre-main-sequence phase, they used a time dependent saturation threshold calculated using the stellar evolution models of Spada et al. (2013). Their XUV evolutionary tracks are shown in Fig. 4. Although we use these tracks in this letter, a set of simple power laws that approximately describe each track can also be found in Tu et al. (2015).

3. RESULTS: THE IMPORTANCE OF STELLAR ROTATIONAL EVOLUTION

By combing the XUV evolution tracks with Eqn. 1 and Eqn. 3, we calculate the evolution of hydrogen atmospheres for planets with core masses between 0.5 and 10 M_{\oplus} , and the initial atmospheric masses between 10^{-5} and 1 M_{pl} . We integrate the atmospheric masses from 10 Myr to 1 Gyr taking into account the time variations in \dot{M}_{at} due to both the stellar XUV evolution and the decreasing R_0 as a result of atmospheric erosion. We stop at 1 Gyr because at that age, F_{XUV} drops well below $100 \text{ erg s}^{-1} \text{ cm}^{-2}$. This is problematic because at low F_{XUV} , the planetary wind at the exobase is slower than the escape velocity (see the middle-left panel of Fig. 1) meaning that many atoms in the flow should return to the planet after traveling on ballistic trajectories in the exosphere.

The cases in our grid break down into four interesting regimes illustrated in Fig. 4 for Earth mass planets with different initial atmospheric masses. In Case A, the initial atmospheric mass ($10^{-4} M_{\oplus}$) is so small that everything is removed very quickly for all rotation tracks. In Case D, the atmosphere ($10^{-1} M_{\oplus}$) is so massive that thermal escape is negligible in all cases. In Case B, the entire atmosphere ($10^{-3} M_{\oplus}$) is removed in all cases, but the time required depends critically on the star's initial rotation rate; for the slow and fast rotators, the atmosphere is removed in 50 Myr and 250 Myr, respectively. The most dramatic difference between the rota-

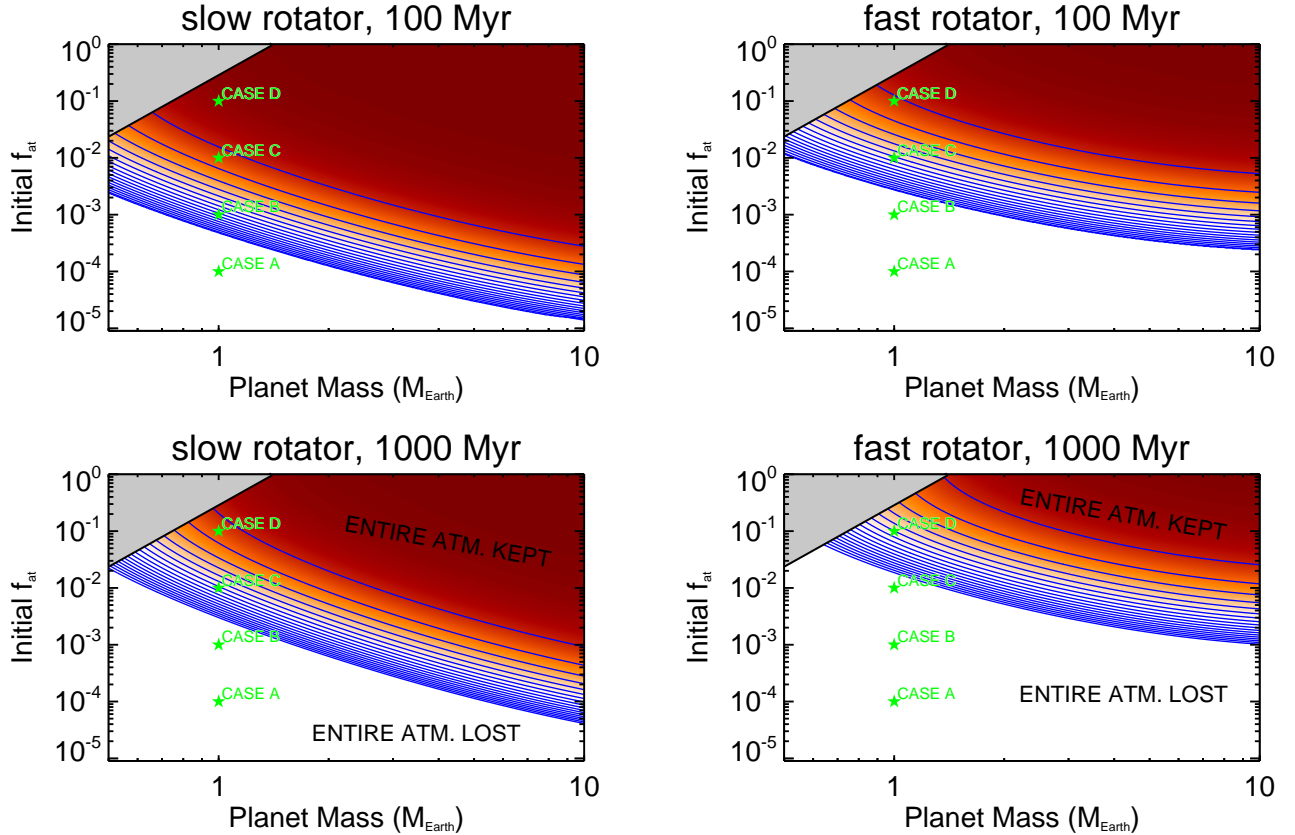


FIG. 5.— Contour plots showing the percentages of the initial hydrogen protoatmospheres remaining at 100 Myr (*upper row*) and 1000 Myr (*lower row*) as a function of planetary mass. In each panel, the contour lines show 20 evenly spaced levels, with dark red and white showing 100% and 0% of the initial atmospheric masses remaining. The left and right columns show the predictions assuming the star is a slow and a rapid rotator, corresponding to the red and blue lines in Fig. 4. The green symbols mark the cases shown in Fig. 4. The grey shaded areas show the region where $f_{\text{at}} > f_{\text{at,max}}$, where $f_{\text{at,max}}$ is estimated from Eqn. 4.

tion tracks is in Case C, where the initial atmospheric mass ($10^{-2} M_{\oplus}$) is such that if the planet is orbiting the rapid rotator, the atmosphere is removed in 400 Myr, whereas if the planet is orbiting the slow rotator, 70% of the atmosphere remains at 1 Gyr. Due to the low stellar activity, the subsequent evolution of the atmosphere is negligible and the hydrogen envelope will never be lost.

In Fig. 5, we show how much atmosphere remains at ages of 100 Myr and 1 Gyr for all planetary masses. The boundary between the regimes where the planet has lost and retained its atmosphere is not only dependent on planetary mass and the age of the system, but also strongly dependent on the initial rotation rate of the host star. The cases shown in Fig. 4 for Earth mass planets are similar for all planetary masses, with the only difference being that the boundaries between the regimes are shifted. The grey shaded areas show where our calculations are unrealistic because low mass planets will not collect and hold onto such massive atmospheres (Lammer et al. 2014; Stökl et al. 2015).

4. DISCUSSION

In this letter, we develop a method for estimating the evaporation of hydrogen atmospheres and give scaling laws that can easily be applied. We show that the initial rotation rate of the central star can be fundamentally important for the evolution of a planetary atmosphere. In all cases, we assume no intrinsic large

scale planetary magnetic field, which could influence the flow and change \dot{M}_{pl} if the gas is highly ionised (Khodachenko et al. 2015). We have also only considered thermal mass loss due to the heating of the upper atmosphere. For hydrogen atmospheres, thermal mass loss dominates (Kislyakova et al. 2013; Kislyakova et al. 2014), and this is also likely to be the case for atmospheres made of heavier species if the XUV energy input is high enough (Tian et al. 2008; Tian et al. 2009). For example, Tian (2015) showed that thermal escape of O_2 from initially H_2O dominated atmospheres can be significant in certain cases. In other cases, the mass loss might be dominated by non-thermal processes such as stellar wind charge exchange and pickup (Lichtenegger et al. 2010). The erosion of non-hydrogen dominated atmospheres therefore depends strongly on stellar winds; easily applicable models for the properties and evolution of stellar winds were given by Johnstone et al. (2015a) and Johnstone et al. (2015b).

Our results provide further confirmation of the conclusions of Lammer et al. (2014) that higher mass habitable-zone terrestrial planets could have difficulty losing hydrogen envelopes if they form in the circumstellar disk. Lower mass terrestrial planets, on the other hand, will lose their hydrogen atmospheres much more effectively. For example, our results indicate that no $\sim 0.5M_{\oplus}$ planets will keep hydrogen atmospheres for more than 1 Gyr regardless of the activity evolutions of their host stars;

this suggests that low-density habitable zone planets with such masses will only be found in young systems.

Although we have only considered hydrogen dominated protoatmospheres, the evolution of stellar rotation is also fundamentally important for the formation and evolution of secondary atmospheres and the development of habitability. For a planet to be habitable, it must first lose its protoatmosphere, and then it must also develop and retain an appropriate secondary atmosphere. Consider a habitable-zone Earth mass planet formed early enough to pick up a substantial hydrogen envelope. The initial rotation rate of the host star not only determines if the planet will lose its protoatmosphere, but also how long this process will take. A rapid rotator might cause this to happen very quickly, whereas a slow rotator might allow the atmosphere to remain for hundreds of Myr, potentially slowing down the solidification of the planet's surface and disrupting the formation of the secondary atmosphere.

Stellar magnetic activity evolves in non-trivial ways

that depend sensitively on the star's rotational evolution. Simple evolutionary decay laws that give one-to-one relations between age and XUV emission or winds are inappropriate at young ages. The aim of this letter, however, is not simply to study the importance of the initial stellar rotation rate on atmospheric evaporation; our results clearly demonstrate that a strong understanding of stellar activity evolution is an essential ingredient in detailed studies of the evolution of planetary atmospheres.

The authors thank the anonymous referee for providing useful suggestions on our manuscript. This study was carried out with the support by the FWF NFN project S11601-N16 "Pathways to Habitability: From Disk to Active Stars, Planets and Life" and the related subprojects S11602-N16, S11604-N16, and S11607-N16. LT was supported by an "Emerging Fields" grant of the University of Vienna through the Faculty of Earth Sciences, Geography and Astronomy. PO and HL acknowledge the FWF project P27256-N27.

REFERENCES

- Bouvier, J., Matt, S. P., Mohanty, S., et al. 2014, *Protostars and Planets VI*, 433
- Chadney, J. M., Galand, M., Unruh, Y. C., Koskinen, T. T., & Sanz-Forcada, J. 2015, *Icarus*, 250, 357
- Erkaev, N. V., Lammer, H., Odert, P., Kulikov, Y. N., & Kislyakova, K. G. 2015, *MNRAS*, 448, 1916
- Erkaev, N. V., Lammer, H., Odert, P., et al. 2013, *Astrobiology*, 13, 1011
- Freedman, R. S., Marley, M. S., & Lodders, K. 2008, *ApJS*, 174, 504
- Gallet, F., & Bouvier, J. 2013, *A&A*, 556, A36
- Güdel, M. 2004, *A&A Rev.*, 12, 71
- Güdel, M., Guinan, E. F., & Skinner, S. L. 1997, *ApJ*, 483, 947
- Herbst, W., Bailer-Jones, C. A. L., Mundt, R., Meisenheimer, K., & Wackermann, R. 2002, *A&A*, 396, 513
- Howe, A. R., Burrows, A., & Verne, W. 2014, *ApJ*, 787, 173
- Ionov, D. E., & Shematovich, V. I. 2015, *Solar System Research*, 49, 339
- Jardine, M., Collier Cameron, A., Donati, J.-F., Gregory, S. G., & Wood, K. 2006, *MNRAS*, 367, 917
- Johnstone, C. P., Güdel, M., Brott, I., & Lüftinger, T. 2015a, *A&A*, 577, A28
- Johnstone, C. P., Güdel, M., Lüftinger, T., Toth, G., & Brott, I. 2015b, *A&A*, 577, A27
- Khodachenko, M. L., Shaikhislamov, I. F., Lammer, H., & Prokopov, P. A. 2015, *ApJ*, 813, 50
- Kislyakova, K. G., Lammer, H., Holmström, M., et al. 2013, *Astrobiology*, 13, 1030
- Kislyakova, K. G., Johnstone, C. P., Odert, P., et al. 2014, *A&A*, 562, A116
- Koskinen, T. T., Harris, M. J., Yelle, R. V., & Lavvas, P. 2013, *Icarus*, 226, 1678
- Kraus, A. L., Ireland, M. J., Hillenbrand, L. A., & Martinache, F. 2012, *ApJ*, 745, 19
- Lammer, H., Lichtenegger, H. I. M., Kulikov, Y. N., et al. 2007, *Astrobiology*, 7, 185
- Lammer, H., Stökl, A., Erkaev, N. V., et al. 2014, *MNRAS*, 439, 3225
- Lichtenegger, H. I. M., Lammer, H., Grießmeier, J.-M., et al. 2010, *Icarus*, 210, 1
- Lissauer, J. J., Fabrycky, D. C., Ford, E. B., et al. 2011, *Nature*, 470, 53
- Lopez, E. D., & Fortney, J. J. 2014, *ApJ*, 792, 1
- Luger, R., Barnes, R., Lopez, E., et al. 2015, *Astrobiology*, 15, 57
- Lundin, R. 2011, *Space Sci. Rev.*, 162, 309
- Lunine, J. I., O'Brien, D. P., Raymond, S. N., et al. 2011, *Advanced Science Letters*, 4, 325
- Marcy, G. W., Weiss, L. M., Petigura, E. A., et al. 2014, *Proceedings of the National Academy of Science*, 111, 12655
- Matt, S. P., Brun, A. S., Baraffe, I., Bouvier, J., & Chabrier, G. 2015, *ApJ*, 799, L23
- Mordasini, C., Alibert, Y., Georgy, C., et al. 2012, *A&A*, 547, A112
- Murray-Clay, R. A., Chiang, E. I., & Murray, N. 2009, *ApJ*, 693, 23
- Rogers, L. A. 2015, *ApJ*, 801, 41
- Sanz-Forcada, J., Micela, G., Ribas, I., et al. 2011, *A&A*, 532, A6
- Saunon, D., Chabrier, G., & van Horn, H. M. 1995, *ApJS*, 99, 713
- Semenov, D., Henning, T., Helling, C., Ilgner, M., & Sedlmayr, E. 2003, *A&A*, 410, 611
- Shaikhislamov, I. F., Khodachenko, M. L., Sasunov, Y. L., et al. 2014, *ApJ*, 795, 132
- Shematovich, V. I., Ionov, D. E., & Lammer, H. 2014, *A&A*, 571, A94
- Spada, F., Demarque, P., Kim, Y.-C., & Sills, A. 2013, *ApJ*, 776, 87
- Stökl, A. 2008, *A&A*, 490, 1181
- Stökl, A., Dorfi, E., & Lammer, H. 2015, *A&A*, 576, A87
- Tian, F. 2015, *Earth and Planetary Science Letters*, 432, 126
- Tian, F., Kasting, J. F., Liu, H.-L., & Roble, R. G. 2008, *Journal of Geophysical Research (Planets)*, 113, 5008
- Tian, F., Kasting, J. F., & Solomon, S. C. 2009, *Geophys. Res. Lett.*, 36, 2205
- Tian, F., Toon, O. B., Pavlov, A. A., & De Sterck, H. 2005, *ApJ*, 621, 1049
- Tóth, G. 1996, *Astrophysical Letters and Communications*, 34, 245
- Tu, L., Johnstone, C. P., Güdel, M., & Lammer, H. 2015, *A&A*, 577, L3
- Vidotto, A. A., Gregory, S. G., Jardine, M., et al. 2014, *MNRAS*, 441, 2361
- Wright, N. J., Drake, J. J., Mamajek, E. E., & Henry, G. W. 2011, *ApJ*, 743, 48